

Investigation of Microstructure and Mechanical Properties of Aluminium 5356 Using Wire Arc Additive Manufacturing

K. Saravanakumar^{1*}, S. Ananth², M. Dharshini³, J. Medoline⁴,
K.M. Sansuuki Priyanka⁵

^{1,2,3,4,5}Department of Production Engineering, PSG College of Technology, Coimbatore, Tamil Nadu

*Corresponding Author Email and Phone Number: ksk.prod@psgtech.ac.in

Article received: 07/11/2023, Article Revised: 19/12/2023, Article Accepted: 30/12/2023

[Doi: 10.5281/zenodo.10523562](https://doi.org/10.5281/zenodo.10523562)

© 2023 The Authors. This is an open access article distributed under the [Creative Commons Attribution License 4.0 \(CC-BY\)](https://creativecommons.org/licenses/by/4.0/), which permits unrestricted use, distribution, and reproduction in any medium, provided the original work is properly cited.

Abstract

Wire arc additive manufacturing is a three-dimensional metal printing method that constructs objects layer-by-layer using an electric arc. This study used a base of Aluminum 6082 alloy to create a multi-layer structure. An automatic gas metal arc welding process was employed, with parameters such as current, stick-out distance, and travel speed. To facilitate the GMAW process, Aluminum 5356 was utilized as filler material. Three-factor and three-level approach was taken for the L9 design of experiments to build a multiwall structure. Pure argon serves as the inert gas in this experiment. The L9 experiment was used to select the optimal parameters. The zig-zag tool path strategy was employed to disperse residual stress and prevent lengthy, continuous weld lines. The liquid penetrant test reveals that samples 1–4 are rejected due to overfill. Samples seven and eight exhibit reduced joint and fatigue strength due to a smaller bead width. The sixth weld bead sample was chosen as the ideal process parameter, showing minimal undercuts and reduced overfills compared to other samples. This research demonstrates the potential of WAAM for creating high-quality multi-layer structures while optimizing process parameters for superior outcomes.

Keywords: Wire arc additive manufacturing, Aluminium 5356 alloy, Gas metal arc welding, Liquid penetrant test, L9 design of experiments.

1. INTRODUCTION

Additive manufacturing technologies can be classified into powder- and wire-based processes, which are established based on the supplements used in additive manufacturing materials. In wire arc additive manufacturing, the filler wire is melted using an electric arc, and the multiwall structure is built layer-by-layer to form a three-dimensional component. WAAM can be more beneficial in the production of enormous components with complicated geometries, and it also reduces reworking through efficient material utilization. Many

metallic materials, such as aluminium alloys and nickel-based superalloys, have been successfully utilized by the WAAM process. Magnesium-based alloys possess high corrosive resistance and heat resistance; these are high-temperature alloys that thereby serve their purpose in the aerospace and nuclear power industries. The aluminum 5xxx series is a family of magnesium-based alloys; among these, aluminum 5356 can endure temperatures up to 500°F without degrading or losing strength. Aluminum is readily weldable, and methods like gas tungsten arc welding (GTAW) or gas metal arc welding (GMAW) can be used for welding aluminium alloys. Nur Izan et al. [1] studied the effects of heat resources and process variables that influence porosity and bead geometry and concluded that a finer microstructure can be obtained with a better cooling rate; a coarser microstructure is obtained with an increase in deposition height due to heat accumulation. Vyskoč et al. [2] studied the impact of filler wire feed rate on butt laser weld joints and concluded that lower feed rates led to increased porosity in the weld metal, particularly without filler wire usage. Maider et al. [3] studied that uniformly distributed microstructure is obtained when there is no interlayer dwell time, and columnar dendrite is formed if there is interlayer dwell time. He concluded that heat treatment is unsuitable for materials with low aging temperatures and time to obtain good mechanical properties. Yuan Bo et al. [4] studied the microstructural and mechanical properties of Aluminium 5356 and stated that rapid cooling resulted in smaller grains, and thus higher tensile strength was obtained as a result. Thus, the mechanical properties of Aluminium 5356 were better than those of the cast materials. Vimal et al. [5] studied that the mechanical properties can be increased by heat treatment up to 450 °C, thus eliminating the β phases. Also, pulsed arc-based gas metal arc welding (GMAW) was the most suitable process to increase efficiency during manufacturing. Pramod et al. [6] studied the applications of aluminium 5052, which are used in marine industries, as it has the property of corrosion resistance with pulsed CMT (cold metal transfer). Zhao et al. [7] studied the aluminium alloy 5356 and demonstrated that the temperature of the melt pool in the center increases as there is an increase in interlayer with the same cooling time. The temperature of the melt pool reduces gradually as the cooling time for the interlayer increases. Sen li et al. [8] studied the effects of shielding gas on aluminium 5356 alloy, stating that the weld beads where argon gas was used as a shielding gas had more advantage over N_2 gas, which showed reduced mechanical properties of strength and plasticity. Jisun et al. [9] studied the conditions of bead geometry by changing the parameters like current, voltage, and feed rate. As a result, a response for deposition efficiency was obtained when there was an increase in heat input. Chuangu Zu et

al. [10] studied the effect of heat input on wall width. Where the wall width increases with increasing the wire feed speed, there is a decrease in wall width when the travel speed decreases. Aldalur et al. [11] used the WAAM technique based on gas metal arc welding GMAW. They produced Al 5356 wire with a diameter of 1.2 mm and compared three working modes namely pulsed GMAW, cold arc, and pulses AC mode. Concluded by newly introducing pulsed AC mode. That reduced porosity by 6 times compared to cold arc and 10 times compared to the GMAW process. Jiankun et al. [12] studied the application of cable-type welding wire (CWW) in WAAM and concluded that CWW produces higher-quality parts with defect-free deposits, equiaxed grains, and significantly improved mechanical properties. Grain morphology and formation of defects were observed through optical microscopy and XRD analyses and defect deposits with equiaxed grains were also formed. Derekar et al. [13] studied the pore distribution with the help of the Computer tomography radiography technique. Additively manufactured aluminum alloy samples were prepared using the direct current pulsed MIG/MAG process. Ming et al. [14] used a workpiece vibration to study the mechanical properties of pores. It induces a stir in the molted pool that suppresses the porosity and removes the fine grain zone. SEM, TEM, and EBSD microstructure were analyzed. It increases the ultimate tensile strength of the samples and exceeds the aluminum wrought alloy. Ying Zhu et al. [15] studied laser shock peening and innovative surface treatment techniques combined with WAAM to refine microstructure, modify residual stress, and enhance tensile properties of aluminum 2391 alloy. Bintao et al. [16] review on WAAM technique to provide a view of the material properties of deposited parts. for the fabricated components analyzed the mechanical properties and microstructure. The defect generated in the process is due to material characteristics and process parameters.

Wahsh et al. [17] used approach pulsed gas metal arc welding (GMAW-P) for deposition. process design improvises the Al-prismatic blocks. Prediction and process optimization models are significant for processing parts free from volumetric defects. Wenji et al. [18] studied the arc sensor which has been used for seam tracking. Pulsed gas metal arc welding process used for manufacturing arc sensing products for T and V-shaped grooves. They investigated the linear characteristics of the mathematical model. This study highlights the P-GMAW arc sensing technology for the improved narrow gap welding process. Ahn et al. [19] investigated the mechanical properties of Aluminum alloy 2024-T3. studied the impact of wire feed rate, revealing that high feed rates over 4.0 m/min caused instabilities, while low feed rate under 2.0 m/min had limited chemical modification of the weld pool. The

use of filler metal enhanced weld quality by reducing defects, promoting ductile fracture behavior, and minimizing micro-hot cracks and porosities. Li et al. [20] studied the continuous tool path generation that uses a combination of zig-zag and contour tool path strategies and as a result, they formed a closed curve by connecting all the combinations of sub-paths. From the survey, filler rod and workpiece are selected. Aluminum 6082 was used as a base plate to build multi-wall layer. Aluminum 5356 alloy is the electrode (filler wire) used for welding, where the diameter of filler wire is 1.2 mm, which results in better aspect ratio. ASTM E-1251 is the standard used in chemical composition testing which is carried out using OES (optical emission spectroscopy). Taguchi L9 DOE (Design of experiments) is chosen for the parameter optimization. Taguchi L9 experiments were carried out with respect to the selected process parameters. Samples with uniform deposition, better width to depth ratio (aspect ratio) are taken as response variables in the selection of optimum process parameters. Liquid penetrant test (LPT) is done to identify the defects (like cracks and pores) present in the material without damaging them. The aim of the work was to identify the weld defects and select optimum process parameters based on weld bead appearance using liquid penetrant test (LPT).

2. EXPERIMENTAL DETAILS

2.1. Workpiece Material

In this experiment, the base plate used is made of Aluminium 6082 alloy with the dimensions of 300 mm × 150 mm × 15 mm. Aluminium 5356 alloy is used as filler wire. For the welding process, a standard electrode with a diameter of 1.2 mm was chosen, although there are other options available, including a 2.4 mm diameter electrode. The decision to use the 1.2 mm wire is based on several factors. Firstly, it produces a higher aspect ratio, i.e. the height of the weld bead is greater compared to its width. This is beneficial for the experiment as it allows for less surface waviness during the fabrication process. This is important as it ensures greater control and precision during the welding process. Aluminum 6082 alloy is composed mainly of aluminum (Al) as the base metal, along with notable quantities of magnesium (Mg). Magnesium alloy is known for its corrosion resistance, blend of strength with other materials, and ease of machining. The significant magnesium content contributes to its strength, making it well-suited for structural purposes. Aluminum 5xxx series alloys shows better and improved results when they are welded with Aluminium 6082. The chemical composition of base plate and filler wire are shown in the Table 1 and Table 2.

Table 1. Chemical composition of the base plate (Aluminium 6082 alloy)

Composition	Si	Fe	Cu	Mn	Mg	Zn	Cr	Ti	Others	Al
Percentage (%)	0.72	0.21	0.27	0.075	0.95	0.001	0.097	0.029	0.096	97.55

2.2. Filler Wire Material

In wire arc additive manufacturing, filler wire is fundamentally utilized to create 3D parts. The desired part is created by melting the wire using an arc and depositing the molten metal on the base plate layer-by-layer. By controlling the wire feed rates, thermal gradients and cooling rates can be improved, resulting in reduced residual stress and distortion in the manufactured part. The chemical composition of Aluminium 5356 alloy is shown in Table.2. The presence of magnesium enhances the overall strength of the alloy, while the other elements contribute to its resistance against corrosion and heat.

Table 2. Chemical composition of the filler wire (Aluminium 5356 alloy)

Composition	Si	Fe	Cu	Mn	Mg	Zn	Pb	Ni	Sn	Ti	Al
Percentage (%)	0.054	0.17	0.007	0.11	4.77	0.001	0.002	0.004	0.0005	0.13	94.55

Gas Metal Arc Welding (GMAW) enables precise regulation of the heat input and offers consistent and controlled heat input, making it highly suitable for welding aluminum 5356, a material prone to heat-related issues. Moreover, it delivers exceptional fusion and penetration when working with aluminum alloys, ensuring strong, reliable welds with good interlayer bonding. This aspect is crucial for additive manufacturing procedures. Additionally, GMAW generates minimal spatter, which proves particularly advantageous in additive manufacturing, as it diminishes the necessity for post-processing and enhances the overall quality of the manufactured components.

2.3. Experimentation

2.3.1. Machine Specifications

The R-30iB/R-30iB software is specifically designed for the FANUC Arc Mate 100iC/12 welding robot. The software enables the robot to perform complex welding tasks with high accuracy and repeatability. The FANUC Arc Mate 100iC/12 shown in Figure 1 is equipped with a welding power source, which is the Fronius TPS 400i LCS advanced

MIG/MAG Inverter Power Source. It is capable of delivering high-quality welds with minimal spatter and excellent penetration. The servo-control units of the Arc Mate 100iC/12 play a crucial role in the robot's movement and control. These units are responsible for controlling the robot's six axes, allowing for smooth and precise motion. The servo-control units ensure that the robot moves with high speed and accuracy, resulting in efficient and effective welding operations. These accessories include an oscillation facility, which allows the robot to perform oscillating welds, creating stronger and more durable welds. The wire snipping facility enables the robot to cut the welding wire at the end of each weld, ensuring clean and precise welds. The torch cleaning facility ensures that the welding torch remains clean and free from any contaminants, preventing defects in the welds. Furthermore, the robot has provisions for mounting additional sensors, allowing for customization and integration of advanced sensing technologies.

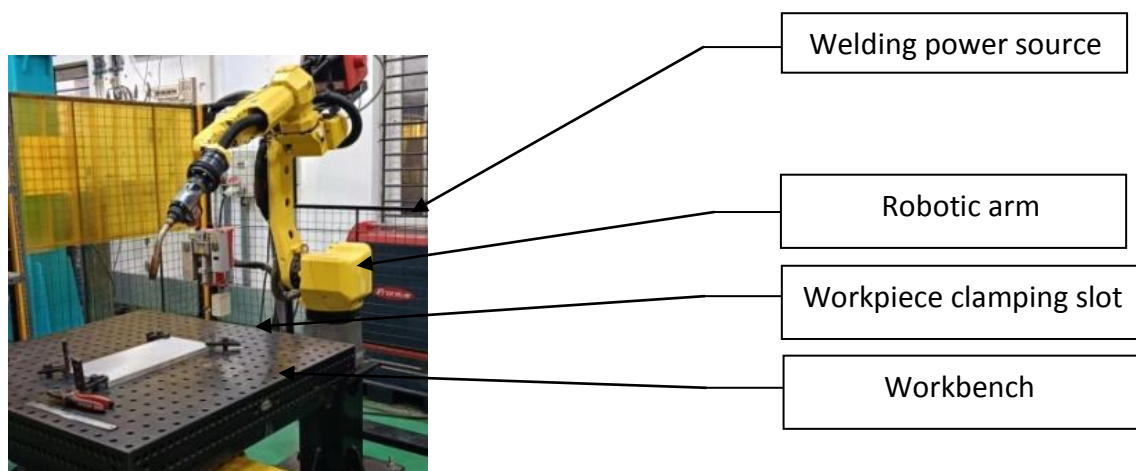


Figure 1. FANUC Arc Mate 100iC/12 – Robotic welding lab

2.3.2. Process Parameters

Electric current is crucial in welding for fusing metals, affecting weld penetration, product quality, and process efficiency. Higher current levels lead to deeper weld penetration and faster welding speeds, while lower levels are suitable for thinner materials. The type of current used also plays a significant role, with DC current providing better control and AC current used for materials like aluminum and magnesium to break up surface oxides. Proper selection and control of current is essential for successful and high-quality welds. Stickout distance in welding is the distance between the electrode's length and the tip of the welding gun or torch. It significantly influences the quality of the weld and affects the electrical resistance within the welding circuit. A shorter distance results in lower resistance, a more

stable arc, and is beneficial for thinner materials and precise welds. It also reduces spatters and improves process stability. A longer distance increases resistance, leading to a broader, less stable arc and better penetration and heat distribution for thicker materials. Stickout distance is a critical parameter that must be adjusted before welding processes to achieve desired arc characteristics and heat input, ultimately affecting weld quality, penetration, and appearance. Travel speed is the rate at which a welding torch moves along a workpiece. Too slow can cause excessive heat input, causing a deep weld puddle, while too fast can result in insufficient heat input, causing poor weld penetration and weak welds. Controlling travel speed is crucial for achieving desired weld penetration, strength, and appearance. An optimum travel speed produces a uniform and better weld bead, while too slow can result in wider, flatter beads with defects like undercuts and overfilled welds. Achieving the optimum travel speed is essential for producing a strong multiwall layer structure.

2.3.3. Factors and Their Levels

Taguchi's design of experiments is utilized to minimize the number of experiments and obtain the optimal welding process parameters. In this context, the factors refer to the independent variables or parameters intentionally varied to examine their impact on the fabricated welding part. These factors typically encompass variables that require optimization. Various factors significantly influence the fabricated part, including current, wire feed rate, travel speed and type of the shielding gas employed. The levels represent the different values or conditions at which each factor is tested during the experiment. Each factor can possess multiple levels, with these levels typically chosen to represent a range of values for the factor. To efficiently study a combination of factors and levels while minimizing the number of experimental runs, the Taguchi Method often employs an orthogonal array. In this case, the levels assigned to the factors are represented by A, B, and C. The experiment involves three factors, namely current (measured in Ampere), stick-out distance (measured in mm), and travel speed (measured in mm/s). Table 3 displays the factors and their corresponding levels for the Taguchi's design of experiments. These levels can be expressed alphabetically as A, B and C.

Table 3. Factors and their levels

S.No	Factors	Symbol	Levels		
			I	II	III
1	Current (Ampere)	A	80	100	120
2	Stick-out distance (mm)	B	10	12	14
3	Travel speed (mm/s).	C	3	4	5

2.3.4. (L9) Taguchi

To minimize defects resulting from oxidation during welding, shielding gas has to be supplied. For this specific experiment, a flow rate of 15 liters per minute of shielding gas containing 100% Argon was utilized as shown in Figure 2. The workpiece used for welding is clamped in the workbench and cleaned with acetone before L9 DOE to remove oil stains and impurities present on the surface of the material. Proper clamping alignment was checked before the welding process. After clamping the workpiece, proper shielding gas flow was checked in the pressure cylinder, before starting the welding process, path planning of the robotic arm was verified using FANUC controllers.

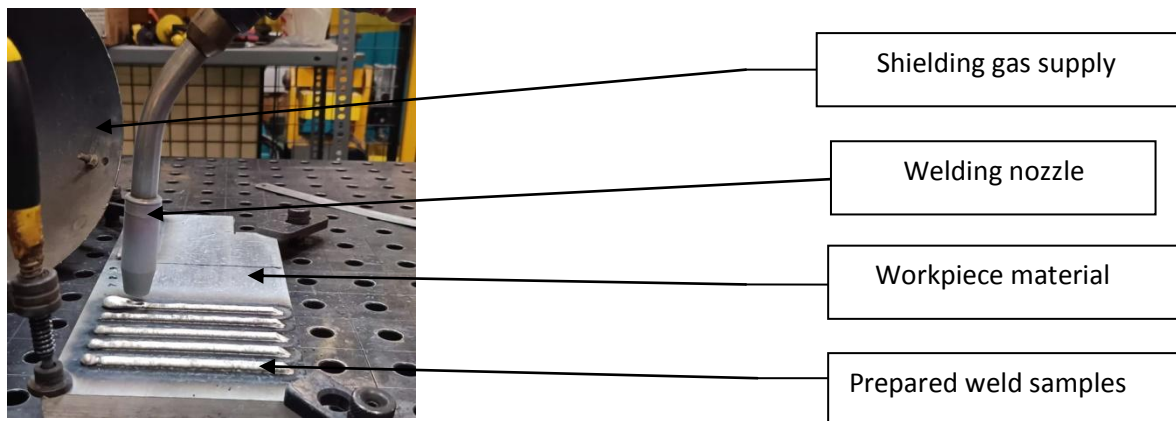


Figure 2. Sample 5 - design of experiments

The weld bead had dwell time for duration of 120s during the trial experiment. A total of nine samples were constructed for the L9 design of experiments, utilizing the parameters listed in Table 4.

Table 4. Taguchi design of experiments (L9)

Sample	Current (Ampere)	Stick out distance (mm)	Travel speed (mm/s)
1	80	10	3
2	100	10	4
3	120	10	5
4	80	12	4
5	100	12	5
6	120	12	3
7	80	14	5
8	100	14	3
9	120	14	4

2.3.5. Tool Path Strategy

Two samples were prepared using a zigzag type tool path strategy with optimum welding parameters. This method ensures uniformity and defect-free structure by overlapping deposition passes between cycles. It also allows for better heat distribution and dissipation, reducing warping risk. The back-and-forth motion of the zigzag pattern ensures thorough mixing of molten metal and better fusion between deposited layers, resulting in strong interlayer bonding and enhanced structural integrity. The pattern disperses residual stresses evenly, avoiding long weld lines and stress concentrations. It also allows for controlled dwell time, reducing defects like porosity. The alternating direction promotes even cooling, preventing hot cracking and improving the metallurgical properties of the welded part.

2.4. Liquid Penetrant Test

Non-destructive testing (NDT) covers a wide range of inspection and testing methods to assess the characteristics of materials while avoiding any harm to the materials when examined. NDT methods do not modify the physical or chemical properties of the material. These techniques find application across diverse industries such as manufacturing, construction, aerospace, and more. These approaches play a vital role in identifying defects without affecting the performance and safety measures of a structure. Liquid penetrant testing is one of the NDT testing methods that use viscous fluid to test the material. The steps followed in liquid penetrant test are shown in Figure 3.

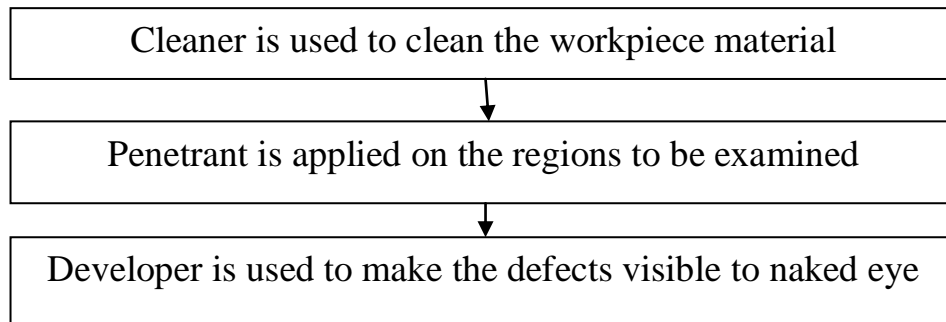


Figure 3. Steps followed in liquid penetrant test

Initially the surface was cleaned by using a cleaning solution. The cleaning process reduces the contaminants present on the surface that could affect the test results after 10 to 15 minutes; penetrant spray was used to spray out the regions which are to be examined. Before the developer is applied, the fluid gets absorbed inside cracks and pores, which allows the penetrant liquid to rise to the surface and give a visible indication of the defect. Then it was allowed to cool, and a liquid penetrant was applied to the surface of the material, which seeps into surface defects. The penetration depends on the dwell time. After the dwell time, the penetrant was removed from the surface of the material through wiping or rinsing. Then the developer was applied to make the defects visible to the naked eye. Figure 4 shows the workpiece material after cleaning using cleaning agent. Figure 5 shows the workpiece material after applying penetrant.

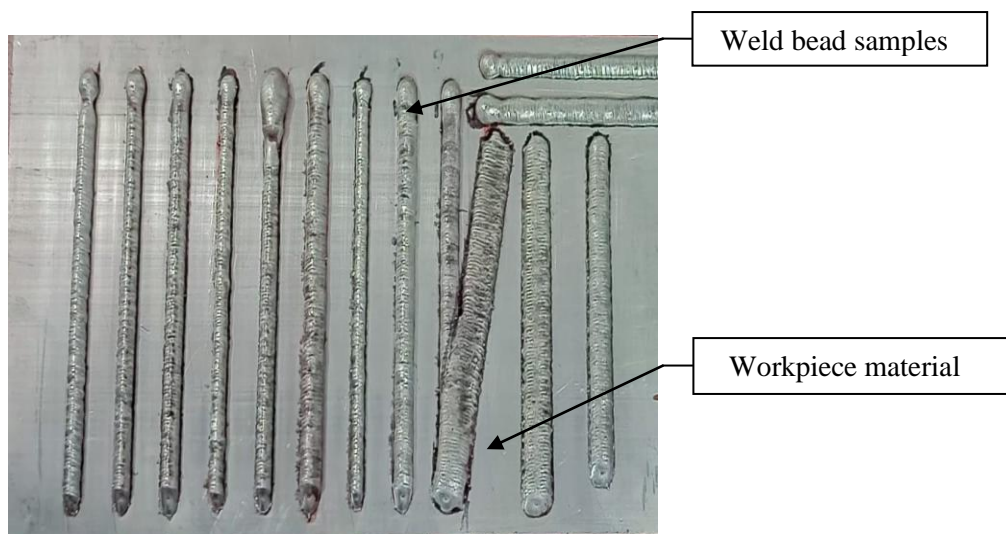


Figure 4. Workpiece material after cleaning

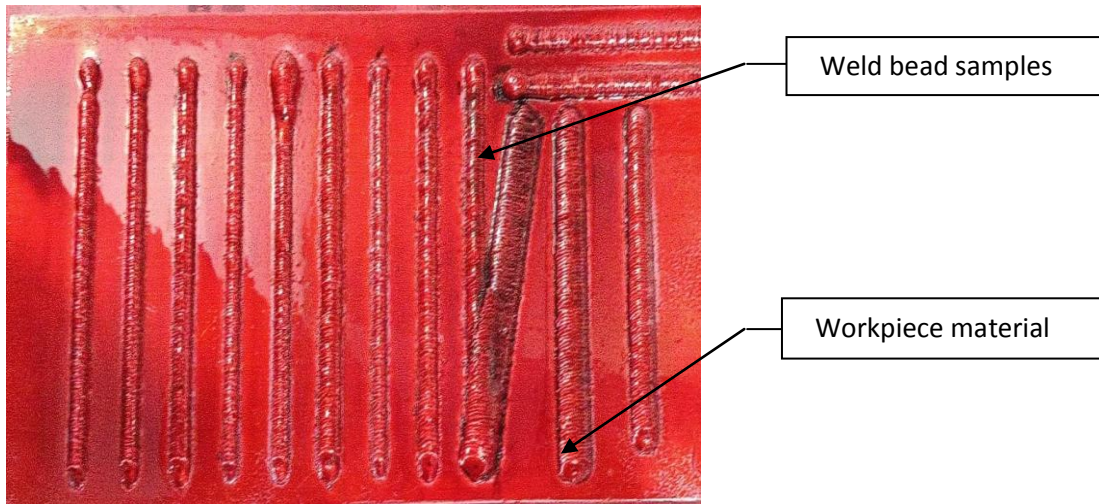


Figure 5. Workpiece material after applying penetrant solution

3. RESULTS AND DISCUSSION

Aluminium 6082 was chosen as the base plate due to its superior weldability with aluminium 5356 alloy. For this experiment, Aluminium 5356 was selected as the filler wire because it has demonstrated improved outcomes when welded with 6xxx series alloys. Gas metal arc welding was determined to be the appropriate process for this experiment as it minimizes defects such as spatter and eliminates the need for post-deposition procedures. The selected factors for this experiment were current (Ampere), stick-out distance (mm), and travel speed (mm/s). The levels for current (Ampere) were 80 Ampere, 100 Ampere, and 120 Ampere, while the stick-out distance (mm) levels were 10 mm, 12 mm, and 14 mm. The travel speed (mm/s) levels were 3mm/s, 4mm/s and 5mm/s. Using the Taguchi L9 orthogonal array, a total of nine experiments were conducted that is shown in Figure 6 and their results are shown in Table 5.

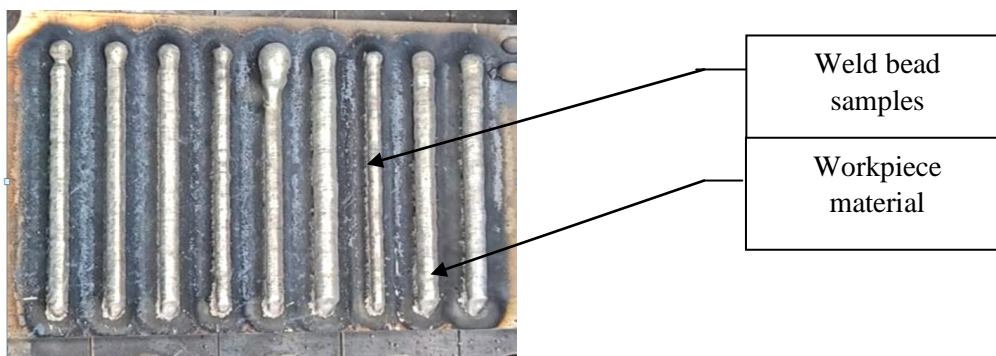


Figure 6. Welded samples using Taguchi (L9) Design of experiment

Some samples exhibited excessive depositions during the initial stage of welding, which could potentially result in weakened wall strength. To address this issue, two samples were prepared using the zig-zag tool path strategy, which yielded better results compared to the samples fabricated using the linear tool path strategy. The zig-zag tool path was employed to reduce stress and prevent cracks.

Table 5. Results of Taguchi design of experiments (L9)

Sample	Current (Ampere)	Stick out distance (mm)	Travel speed (mm/s)	Samples	Defects
1	80	10	3		Overfill
2	100	10	4		Overfill
3	120	10	5		Overfill
4	80	12	4		Overfill
5	100	12	5		Over Deposition
6	120	12	3		Optimum bead
7	80	14	5		Inadequate width
8	100	14	3		Surface waviness
9	120	14	4		Surface waviness

The samples with a wall width size of 8 mm -12 mm are considered, taking into account reduced surface waviness and over deposition. Some samples experienced over deposition, while others had poor weld width size, which could lead to over pouring and reduced wall strength. The zig-zag pattern employed in this strategy allows for improved heat distribution and dissipation, thereby reducing the risk of warping. The back-and-forth motion of the zig-zag pattern ensures thorough mixing of the molten metal and enhances fusion between deposited layers. As a result, strong interlayer bonding is achieved, enhancing the overall structural integrity of the fabricated part. Furthermore, this pattern disperses residual stresses more evenly throughout the part and avoids the formation of long, continuous weld lines, thereby minimizing the risk of stress concentrations or cracking. The zig-zag pattern often involves overlapping the deposition passes, ensuring that there are no gaps or un-fused areas between passes. This overlapping creates a more uniform and defect-free structure.

Additionally, the zig-zag pattern allows for controlled dwell time, ensuring that the deposited material has sufficient time to solidify before additional material is added. This controlled solidification process helps to reduce the risk of defects such as porosity. Moreover, the alternating direction of the zig-zag pattern promotes even cooling, which is crucial for preventing hot cracking and improving the microstructure of the fabricated part. Table 6 shows the three parameters have to be considered before welding samples with zig-zag type tool path strategy those are dwell time, frequency and amplitude.

Table 6. Process parameters for zig-zag type tool path strategy

Parameters	Sample 1	Sample 2
Dwell time (sec)	0.01	0.01
Amplitude (mm)	6	4
Frequency (Hz)	4	4

The parameters utilized for welding samples with a zig-zag type tool path strategy are presented in Table 5. The dwell time refers to the duration between the peak and valley points in the sine wave pattern, which is also known as the sine-wave type tool path. The amplitude is the distance between the horizontal and vertical positions of the tool, while the frequency is the time required for the tool to complete one cycle. These parameters can be easily defined by utilizing the sine wave.

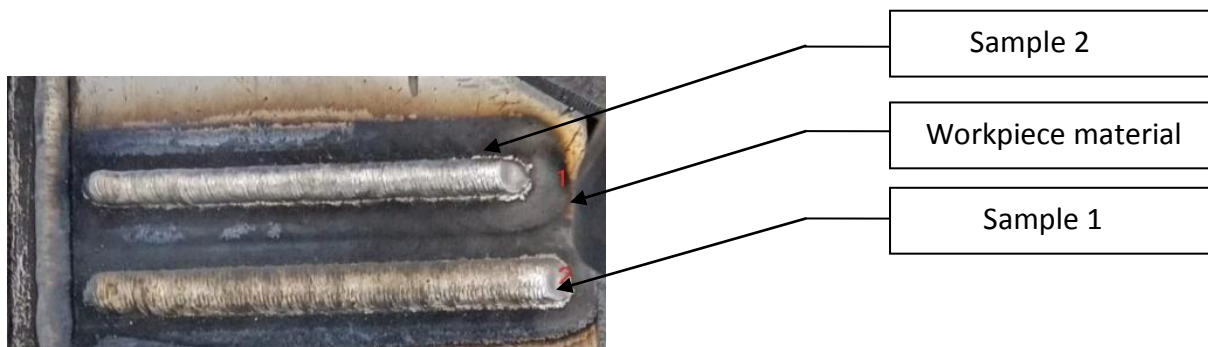


Figure 7. Samples prepared using zig-zag tool path strategy

Here the sample 1 was prepared with amplitude of 6 mm which clearly increased the weld bead width size more than required and it is observed that increased bead width resulted in reduced bead depth which reduces aspect ratio of the fabricated part. Figure 6 clearly infers the above statement. After performing (L9) DOE liquid penetrant test is carried out. Initially the surface was cleaned by using a cleaning solution. The cleaning process reduces the contaminants present on the surface that could affect the test results after 10 to 15 minutes,

penetrant spray is used to spray out the regions which are to be examined. Before the developer is applied, the fluid gets absorbed inside cracks and pores, which allows the penetrant liquid to rise to the surface and give a visible indication of the defect. Then it is allowed to cool, and a liquid penetrant is applied to the surface which seeps into surface defects. The penetration depends on the dwell time. After the dwell time, the penetrant is removed from the surface through wiping or rinsing. Then a developer is applied to make the defects visible to the naked eye. Figure 8 and Figure 9 shows the results of liquid penetrant test.

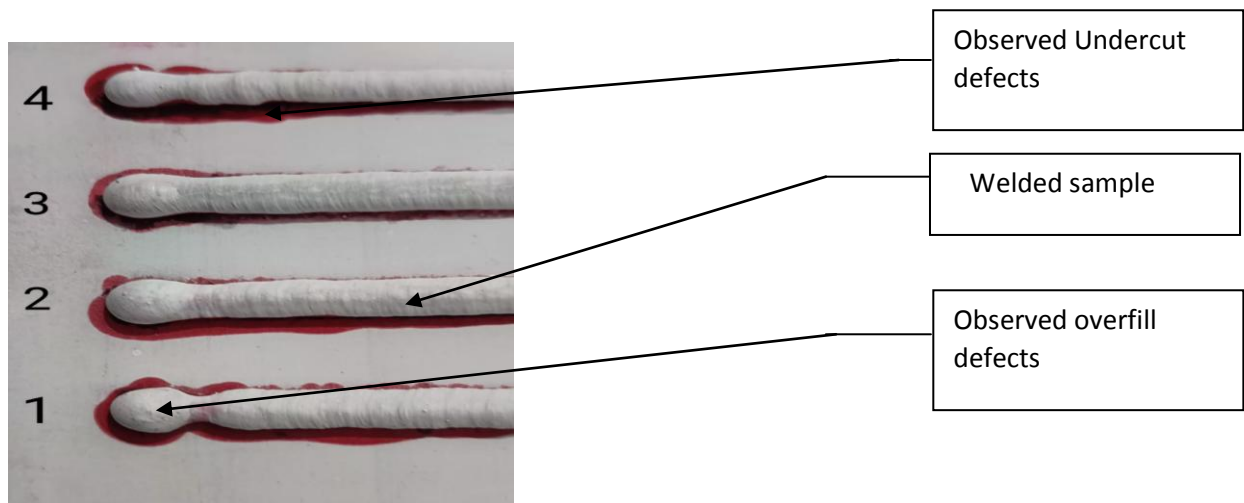


Figure 8. LPT results and discussions

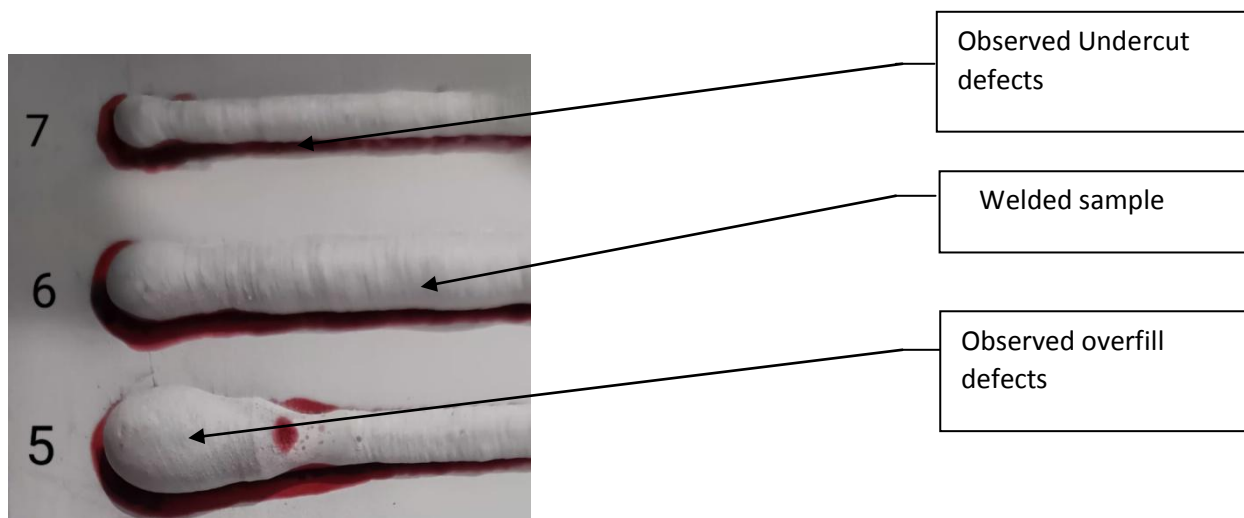


Figure 9. LPT results and discussions

Some samples resulted in over depositions in the initial stage of welding, which may result in poor wall strength, thus two samples were prepared by using zig-zag tool path strategy which merely produced better results comparing the samples fabricated with linear tool path strategy, zig-zag type tool path is followed in order to reduce stress and avoid cracks.

4. CONCLUSION

Based on the LPT results and findings, it is evident that some welded samples exhibit excessive deposition along the welding direction, resulting in an uneven surface. This lack of uniformity can negatively impact the aspect ratio, leading to unsatisfactory outcomes. Moreover, the seventh weld bead displays inadequate width, which is suboptimal for achieving the desired wall width for building multiwall layer structure. These observations emphasize the need for careful consideration and adjustment to ensure optimal welding conditions and strengthen the overall quality of the finished product. In relation to the eighth and ninth samples, surface waviness is observed along the tool path. Overfill defects are identified in the samples 5, 7 and 1, which occurs when metal welded in place exceeds the amount that is really required for the job, these type of defects are caused due to slow travel speed. As a result of this LPT it is found that sample 6 have minimal level of undercuts while comparing with other samples. Sample 6 has reduced overfills comparing with other samples, therefore sample 6 is chosen as the optimum welding process parameter.

Acknowledgement/Funding Acknowledgement

The author(s) received no financial support for the research, authorship, and/or publication of this article.

Declaration of Competing Interest

The authors declare that they have no known competing financial interests or personal relationships that could have appeared to influence the work reported in this paper.

REFERENCES

- [1] Hussein, N. I. S., Ket, G. C., Rahim, T. A., Ayof, M. N., Abidin, M. Z. Z., & Srithorn, J. (2023). Process and Heat Resources for Wire Arc Additive Manufacturing of Aluminium Alloy ER4043: A Review. *Journal of Mechanical Engineering (1823-5514)*, 20(1).
- [2] Vyskoč, M. (2023). Effect of Filler Wire Feed Rate on the Formation of Porosity in Laser Welded Joints of Magnesium Alloy AZ31B–H24. *Metals*, 13(3), 460.

- [3] Arana, M., Ukar, E., Rodriguez, I., Aguilar, D., & Alvarez, P. (2022). Influence of deposition strategy and heat treatment on mechanical properties and microstructure of 2319 aluminium WAAM components. *Materials & Design*, 221, 110974.
- [4] Jiangang, P., Bo, Y., Jinguo, G., Liang, Z., & Hao, L. (2022). Influence of arc mode on the microstructure and mechanical properties of 5356 aluminum alloy fabricated by wire arc additive manufacturing. *Journal of Materials Research and Technology*, 20, 1893-1907.
- [5] Vimal, K. E. K., Srinivas, M. N., & Rajak, S. (2021). Wire arc additive manufacturing of aluminium alloys: A review. *Materials Today: Proceedings*, 41, 1139-1145.
- [6] Vishnukumar, M., Pramod, R., & Kannan, A. R. (2021). Wire arc additive manufacturing for repairing aluminium structures in marine applications. *Materials Letters*, 299, 130112.
- [7] Zhao, P., Fang, K., Tang, C., Niu, J., & Guo, M., "Effect of interlayer cooling time on the temperature field of 5356-TIG wire arc additive manufacturing," *China Welding.*, 30(2), 17-24.
- [8] Li, S., Zhang, L. J., Ning, J., Wang, X., Zhang, G. F., Zhang, J. X., Na, S.J. & Fatemeh, B. (2020). Comparative study on the microstructures and properties of wire+ arc additively manufactured 5356 aluminium alloy with argon and nitrogen as the shielding gas. *Additive Manufacturing*, 34, 101206.
- [9] Lee, H. K., Kim, J., Pyo, C., & Kim, J. (2020). Evaluation of bead geometry for aluminum parts fabricated using additive manufacturing-based wire-arc welding. *Processes*, 8(10), 1211.
- [10] Su, C., Chen, X., Gao, C., & Wang, Y. (2019). Effect of heat input on microstructure and mechanical properties of Al-Mg alloys fabricated by WAAM. *Applied Surface Science*, 486, 431-440.
- [11] Aldalur, E., Suárez, A., & Veiga, F. (2021). Metal transfer modes for Wire Arc Additive Manufacturing Al-Mg alloys: Influence of heat input in microstructure and porosity. *Journal of Materials Processing Technology*, 297, 117271.
- [12] Wang, J., Shen, Q., Kong, X., & Chen, X. (2021). Arc additively manufactured 5356 aluminum alloy with cable-type welding wire: microstructure and mechanical properties. *Journal of Materials Engineering and Performance*, 30(10), 7472-7478.
- [13] Derekar, K., Lawrence, J., Melton, G. B., Addison, A., Zhang, X., & Xu, L. (2019, February). Influence of interpass temperature on wire arc additive manufacturing (WAAM) of aluminium alloy components. In *MATEC Web of Conferences* (p. 5001). EDP Sciences.
- [14] Zhang, C., Gao, M., & Zeng, X. (2019). Workpiece vibration augmented wire arc additive manufacturing of high strength aluminum alloy. *Journal of Materials Processing Technology*, 271, 85-92.
- [15] Sun, R., Li, L., Zhu, Y., Guo, W., Peng, P., Cong, B., ... & Liu, L. (2018). Microstructure, residual stress and tensile properties control of wire-arc additive manufactured 2319 aluminum alloy with laser shock peening. *Journal of Alloys and Compounds*, 747, 255-265.

- [16] Wu, B., Pan, Z., Ding, D., Cuiuri, D., Li, H., Xu, J., & Norrish, J. (2018). A review of the wire arc additive manufacturing of metals: properties, defects and quality improvement. *Journal of manufacturing processes*, 35, 127-139.
- [17] Wahsh, L. M., ElShater, A. E., Mansour, A. K., Hamdy, F. A., Turky, M. A., Azzam, M. O., & Salem, H. G. (2018). Parameter selection for wire arc additive manufacturing (WAAM) process. *Mater. Sci. Technol*, 78-85.
- [18] Liu, W., Li, L., Hong, Y., & Yue, J. (2017). Linear mathematical model for seam tracking with an arc sensor in P-GMAW processes. *Sensors*, 17(3), 591.
- [19] Ahn, J., Chen, L., He, E., Davies, C. M., & Dear, J. P. (2017). Effect of filler metal feed rate and composition on microstructure and mechanical properties of fibre laser welded AA 2024-T3. *Journal of Manufacturing Processes*, 25, 26-36.
- [20] Ding, D., Pan, Z., Cuiuri, D., & Li, H. (2014). A tool-path generation strategy for wire and arc additive manufacturing. *The international journal of advanced manufacturing technology*, 73, 173-183.